LOCAL REGION-BASED ACM WITH FRACTIONAL CALCULUS FOR BOUNDARY SEGMENTATION IN IMAGES WITH INTENSITY INHOMOGENEITY

Norshaliza Kamaruddin[1], Nor Aniza Abdullah[2], Rabha W. Ibrahim[3]

[1, 2] Faculty of Computer Science & Information Technology
University of Malaya, 50603 Kuala Lumpur, Malaysia

[3]Institute of Mathematical Sciences, University of Malaya, 50603Kuala Lumpur, Malaysia

Email: shaliza.kama@yahoo.com[1], noraniza@um.edu.my[2], rabhaibrahim@yahoo.com[3]

ABSTRACT

This study proposes a novel local region-based active contour model (ACM) for image segmentation based on fractional calculus with consideration of the Riemann–Liouville operators. The proposed method aims to achieve accurate boundary segmentation in the presence of severe intensity inhomogeneity. The strength of fractional calculus is exploited with Gaussian Kernel namely, Fractional Gaussian Kernel (FGK) that provides an effective method of edge detection and has good noise immunity. An adaptive window mechanism with various sizes and orientations is employ to maintain and enhance image details especially at the object's boundary and angle. The powerful combination of adaptive window and Fractional Gaussian Kernel (AFGK) provide an efficient way to utilize image information in local regions. Specifically, the fractional differential Heaviside function (FDH) extracts the image gradient and its various intensities for an accurate boundary segmentation outcome. Experiments on both synthetics and medical images demonstrate that the proposed local region-based ACM including fractional calculus realizes accurate boundary segmentation on images even under the most challenging situations, such as severe intensity inhomogeneity interface.

Keywords: active contour model, fractional calculus, adaptive windows, fractional Gaussian kernel, fractional-order derivatives

1.0 INTRODUCTION

Accurate boundary segmentation is one of the biggest challenges in image segmentation, especially the challenges in handling image noise and intensity inhomogeneity problem [1, 2, 3]. Image noise is the "unwanted signals" that appeared in many images [1, 2]. When the level of noise increases, it becomes difficult to obtain satisfying segmentation result. Intensity on the other hand is referring to the level of gray-scale in each individual pixel of an image [5, 6, 7]. Medical images are often affected with distribution of intensity that is not homogeneous, a condition better known as intensity inhomogeneity. High level of intensity inhomogeneity in medical images will create leakage at object's boundary [5, 6]. Boundary leakage is a problem created by weak or missing edges. Intensity inhomogeneity also creates complex texture in medical images [1, 2, 3].

For the past decade, numerous methods have been proposed to accurately segment medical images for the purpose of detecting abnormalities such as tumors or cancerous cells. Among the segmentation methods that have been developed, Active Contour Model (ACM) appears to be the most popular for segmenting medical images [8, 9]. ACM was initially developed by Kass, Witkin and Terpozoulos (1986) and it is classified as edge-based ACM. Even though edge-based ACM can segment some medical images, its result is hardly satisfying [9, 10]. This is because the technique works on image's gradients therefore its success depends on the visibility of edges in an image. Unfortunately, medical images are mostly affected by visual noises that weaken those edges [10, 11].

To address this deficiency, a region-based ACM was developed [12, 13]. The method has proven more successful than edge-based ACM in segmenting noisy medical images due to it robustness in handling noise. However, apart

from the visual noises, many medical images such as MRI and ultrasound are also impaired with intensity inhomogeneity problem [11, 13, 14]. Intensity inhomogeneity is a problem where the distribution of the intensity level in a region of an image is not the same or homogeneous. This condition creates many unwanted segmented areas within a region, a situation better known as oversampling.

Neither edge-based nor region-based ACM method alone can accurately segment medical images with intensity inhomogeneity [14, 16, 17]. In the attempt to resolve this problem, a combination of edge-based and region-based ACM methods were later introduced by many researchers [22]. Some of the hybrid techniques perform better than others in segmenting certain medical images but none has yet able to accurately segment the object's boundary in the presence of intensity inhomogeneity without producing excessive over sampling effect. Moreover, most of these techniques trapped at the local minima problem that leads to inaccurate segmentation outcome.

The local minima problem often occurs in medical images with high level of intensity inhomogeneity. A solution to this situation is to embed the local image information to extract the object boundary. Several studies on ACM have attempted to solve the local minima problem in order to achieve accurate boundary segmentation even in the presence of intensity inhomogeneity. Many local region-based ACM methods are currently attempting to solve the local minima problem. The idea began with the work of Brox and Cremers [18] that extended the Mumford-Shah (MS) model by embedding the local energy as the first-order approximation [15]. The work provided smoother regions by modelling each region with an estimated mean into a local Gaussian neighbourhood. Shawn Lankton [20] conducted experiments that enabled region-based energy to be localized in a variation manner. His work significantly improved the accuracy of heterogeneous image segmentation.

Li et al. [7] analyzed the localized energy and developed a method called local binary fitting energy (LBF). Their work introduced the local energy with a kernel function to extract the local image information and achieve accurate segmentation in the presence of intensity inhomogeneity. Their method yielded good performance in the segmentation process, especially on medical image segmentation. However, the method required high computational cost, especially in handling severe intensity inhomogeneity images. This is because it had to be performed in four convolution operations. Furthermore, sometimes it did not reveal accurate segmentation at the desired object boundary [19,20,21].

Li et al. [26] also developed a novel region-based ACM that derived a local intensity clustering property of the image intensities. The method is therefore named as local intensity clustering (LIC). Based on the image intensities, a local clustering criterion function is defined for the image intensities in a neighbourhood of each point. The function is then integrated to the neighbourhood centre to give a global criterion for image segmentation. The LIC method can be considered as a locally weighted *K*-means clustering method. The method does not consider the clustering variance, which may cause inaccurate segmentation.

Wang et al. [27] developed a new region-based ACM that utilized the local image intensities. The local image intensities are then described by Gaussian distribution with different means and variance as its variables. The means and variances of local intensities are considered as spatially varying functions to handle intensity inhomogeneities and noise of spatially varying strength. As the method highly depending of the means and variances of the Gaussian distributions, small intensities values within the image are not extracted thus it can lead to inaccurate segmentation. In addition, the method provides high computational cost and slow segmentation speed.

Lastly, Darolti et al. [23] proposed a method called local region descriptor (LRD) to characterize the entire image region that had overlapping pixel intensities. The method aimed to solve the problem of overlapping pixels leading to the difficult extraction of the local image information at the object boundary. However, the LRD method has several drawbacks. For instance, its level set evolution acted locally because the Dirac function used was restricted to neighbourhood pixels around the zero level set, and as the consequence, the contour can easily stuck at the local image details. Moreover, the region descriptor used in the LRD method did not consider the region variance, which led to inaccurate segmentation.

Our study presents a novel local region-based ACM for image segmentation based on fractional calculus. We aim to provide accurate boundary segmentation outcome even in the presence of intensity inhomogeneity. In our proposed method, the normal Gaussian filter used in previous ACM methods is now replace with Fractional Gaussian Kernel

(FGK) which considers the capability of nonlinear diffusion function. The strength of the FGK which is nonlinear is used in the proposed method to enhance and maintain the image structure while reducing the image noise. Furthermore, FGK helps to classify and merge the local image information that belongs to the same intensity level [24,25]. An adaptive window is used to give an excellent result to provide a smooth image texture. The window size and orientation vary and adaptively change according to the gradient magnitude in an image. Unlike the normal adaptive window mechanism, the proposed adaptive window is able to move within the critical angle of an object due to the implementation of fractional calculus. In the proposed method, the integer-order gradient operator implemented in most ACM methods is now generalized to fractional differential Heaviside function (FDH) based on energy formulation regulations. The FDH function offers nonlinear protecting capability to maintain the image structure, and has the ability to extract the local image information. The integer-order gradient operator in most ACM methods only weights the image gradient. However, the FDH function weights both image gradient and intensity values to mitigate the local minima problem and improve the object boundary segmentation outcome. The proposed FDH function works within the level set framework. When its energy is minimized at the object boundary, the movement of a contour will stop.

Several research contributions are derived from this work. The proposed method shows several advantages. First is the Adaptive Fractional Gaussian Kernel (AFGK) technique introduces a new method for enhancing image quality within an environment of high level of intensity inhomogeneity. The enhancement is carried out by reducing image noise and enhancing image details. Besides, the AFGK has the capability in merging and grouping the inhomogeneous object in a region. Secondly, the FDH function extracts the image gradient and its various intensities for an accurate boundary segmentation outcome. Lastly, the implementation of fractional-order gradient throughout the proposed model ensures contour stability when manoeuvring every object boundary within the difficult intensity inhomogeneity interface. Furthermore, it also forbids the contour from stopping until the segmentation process is successfully completed. Section 2.0 presents the background of the related methods and algorithms. The review on intensity inhomogeneity in medical images is also discussed in this section. Section 3 describes the proposed method, followed by the experimental results and analysis in Section 4. Section 5 concludes the findings and provides suggestions for future work.

2.0 BACKGROUND

Medical images are low in quality due to visual artefacts such as noise and intensity inhomogeneity. In recent years, a number of ACM methods have started introducing strategies and techniques to reduce the intensity inhomogeneity problem in order to achieve accurate segmentation outcome. Fig. 1 illustrates several images that are affected with noises and intensity inhomogeneity.

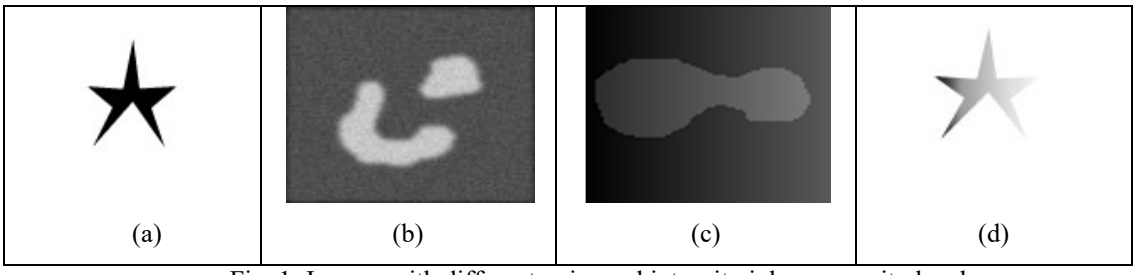

Fig. 1: Images with different noise and intensity inhomogeneity levels

Fig. 1(a) displays an image without noise or intensity inhomogeneity issues. The black star object and the white background represent the homogeneous intensity. The image slightly suffers from blur edges at its boundary. Many ACM methods that utilize local image information are able to successfully segment this kind of image. Fig. 1(b) illustrates an image that suffers from noise in both its foreground and background image. However, both the foreground and background intensities are uniformly distributed. Hence, this situation is not critical because the ACM methods can still manage to segment the image successfully. In contrast, the image in Fig. 1(c) is not affected by noise, but it has an inhomogeneous intensity distribution for both its background and foreground images. Similarly, the image in Fig. 1(d) has severe intensity inhomogeneity issue. Its foreground image intensity decreases

and almost disappears into the background image, particularly on the right side of the star object. In this case, neither the edge- nor the region-based ACM can segment the star object shown in Fig. 1(d). The image condition shown in Fig. 1(d) makes the segmentation process becomes very challenging, and this often occurs in most medical images.

Let Ω be the image domain, and $I(x)$: Ω be the given image. Consider $n(x)$: Ω as the given noise in an image, and $T(x)$: Ω as the true signal to be restored. Let $h(x)$: Ω represent the intensity inhomogeneity because the image has an intensity inhomogeneity problem. We consider the following equation for an image with noise and intensity inhomogeneity:

$$I(x) = h(x)T(x) + n(x) \tag{1}$$

Most medical images are represented by $I(x)$[Eq.(1)]. The segmentation process aims to classify the inhomogeneous object in a region represented by $h(x)$and reduces the image noise given by $n(x)$. The signal represented by $T(x)$ is restored to achieve accurate boundary segmentation. Contour C is obtained to separate a region into homogeneous objects and segment the image according to the ACM method. Following the piecewise smooth method by Mumford–Shah, the image is separated into Ω_1, Ω_2 ....to improve the classification and segmentation result. However, this causes the separation to be trapped in the local minima problem since the method is non-convex. The equation of Mumford–Shah is given as follows:

$$E^{MS}(u, C) = \int_{\Omega} (I - u)^2 \, dx + \mu \int_{\Omega/C} |\nabla u|^2 \, dx + \nu |C| \tag{2}$$

where μ and $\nu > 0$ are fixed parameters, and $|C|$ is the contour length. Because the method is classified as a non-convex, minimizing contour C may be difficult. A similar situation is experienced with the C–V method [7]. Unlike other region-based ACMs, Li et al. utilize the local image information to segment the object boundary in the intensity inhomogeneity region [6]. Their LBF method introduces a kernel function for a scrupulous extraction of the local image information to locate the object boundary. The complete equation for the LBF method is as follows:

$$\begin{aligned} &\varepsilon_x^{LBF}(\phi, f_1(x), f_2(x)) \\ &= \lambda_1 \int K_\sigma(x - y)|I(y) - f_1(x)|^2 H\big(\phi(y)\big)dy \\ &+ \lambda_2 \int K_\sigma(x - y)|I(y) - f_2(x)|^2 (1 - H\big(\phi(y)\big))dy \end{aligned} \tag{3}$$

whereλ_1 and λ_2 are two positive constants. K is a kernel function with a localization property in which $K(u)$ decreases and approaches zero as |u| increases. $f_1(x)$ and $f_2(x)$ are numbers that fit the image near point x [7]. The kernel function used in this method is based on the Gaussian kernel and is given as:

$$K_\sigma(x) = \frac{1}{(2\pi)^{n/2}\sigma n} e^{-|x|^2/2\sigma^2} \tag{4}$$

The integral $\varepsilon_x^{LBF}$is minimized to segment the entire segmented object boundary accurately. Moreover, the fitting values of f_1 and $f_2$are optimally chosen. However, an image becomes more blurry when the Gaussian value parameter increases due to the classification of the LBF as a linear function. This situation results in the loss of critical information, especially at the object boundary. On the other hand, the local Gaussian distribution (LGD) improves the LBF method using the Gaussian distribution with different means and variances to describe the local image intensities. The energy minimization is achieved by employing an interleaved level set evolution and estimation of local intensity means and variances in an iterative process [7]. The minimization algorithm is given as follows:

$$E_X^{LGDF} = \sum_{i=1}^{N} \int_{\Omega_1 \cap \vartheta_x} -log\ _{i,x}(I(y))dy \tag{5}$$

The method assumes that the local Gaussian distribution mean and variance are spatially varying parameters, which gives the following equation:

$$p_{i,x}\,(I(y)) = \frac{1}{\sqrt{2\pi\sigma_i(x)}} \exp\left(-\frac{(u_i(x) - I(y))^2}{2\sigma_i(x)^2}\right) \tag{6}$$

where $u_i(x)$ and $\sigma_i(x)$ are the local intensity means and standard deviations, respectively. One of the disadvantages of the LGD is its contour movement instability. This instability is caused by high utilization of the local property which gives rise to the local minima problem. Therefore, the LGD is suitable for the segmentation of a medical image with less intensity inhomogeneity problem.

3.0 THE PROPOSED METHOD

This section presents the design and development of a novel local region-based ACM that uses fractional calculus in its implementation. The proposed method is an automatic segmentation approach that is based on the ACM concept, and is classified under the spatial domain. The goal of the method is to minimize the energy at the contour location in the object boundary position, where the energy is minimized based on the level set framework. The FGK is used in the proposed method to enhance the image texture and maintain its structure. In the previous ACM method, as the normal Gaussian filter is used, the loss of image information occurs as the parameter increases. As the consequence, the image becomes unclear.

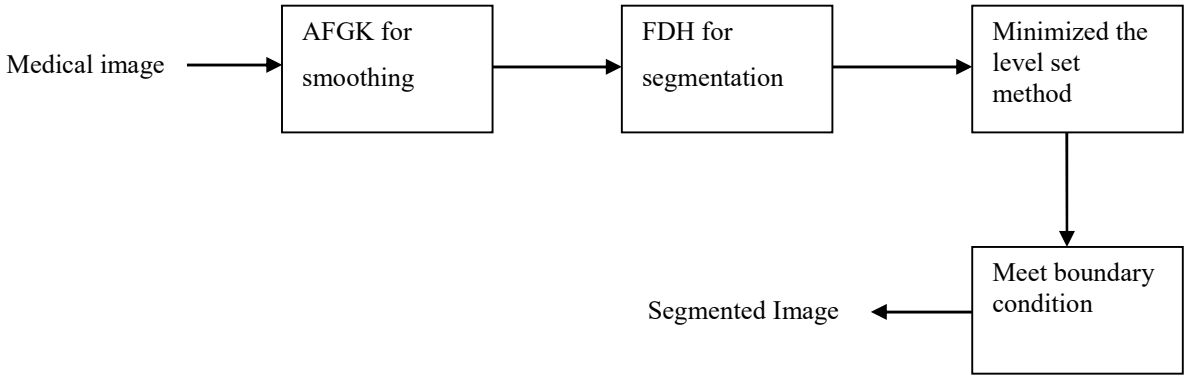

Fig. 2: Process flow of the proposed method

In the proposed method, as the Gaussian kernel is used with the strength of fractional calculus, the detailed image, which includes critical information is maintained regardless of the increased of the parameter. The FGK also improves the classification of the inhomogeneous objects in a region. In addition to that, the Gaussian kernel embeds the local image information within the region to extract the object boundary during the segmentation process. An adaptive rectangular window with variant sizes and orientations is also used to obtain an excellent result in providing smooth image texture. The rectangular window moves throughout the image to enhance and maintain the image texture. The implementation of the window mechanism in the proposed method does not have specific sizes as it depends on the topology changes in the image. Furthermore, the implementation of the fractional calculus

controls the rectangular window movement across the image to achieve accurate segmentation. The window movement is particularly controlled within the critical area of the segmented object, which includes the object boundary angle. This technique is called Adaptive Fractional Gaussian Kernel (AFGK) because an adaptive window mechanism is applied with FGK to enhance the image texture. The parameters used in this process are discussed in Section 3.1. In the proposed method the integer-order gradient operator is generalized to fractional differential Heaviside function. The integer-order gradient operator is normally used to extract the gradient information in an image for improved segmentation. However, it only weighted the gradient and ignored the intensity of the image. The fractional differential Heaviside (FDH) function used in the proposed method has the ability to protect the image details and the lower frequency in an image. Moreover, it is also capable of extracting both the image gradient and intensity to improve the segmentation outcome. Extracting the local image information at the object boundary is highly needed to obtain accurate boundary segmentation. Accordingly, the FDH function is implemented within the level set method framework where it is minimized once the condition is satisfied. Fig. 2 illustrates the process flow to summarize the entire process of the proposed method.

3.1 AFGK

The AFGK technique is implemented in the proposed method with the aim to provide a smooth image texture with less noise and maintain image details. The smooth image texture enables the rapid movement for the contour evolution toward the object in the image. The applications of Gaussian filter in the previous ACM methods are based on the linearity diffusion function. As a consequence, the image becomes blurry each time the Gaussian parameter increases. We proposed the use of FGK on the basis of nonlinear diffusion to mitigate the situation. The nonlinear diffusion is capable of maintaining the image structures. Accordingly, the edge is preserved to achieve a better segmentation outcome. An adaptive rectangular window is used with the FGK to further maintain the image details. The adaptive window varies in size and orientation to easily adapt to the change in the image gradient or intensity. The rectangular window moves through the image with the goal of retaining the image structure while removing or reducing the random image noise. In a region with inhomogeneous objects, the adaptive window with the capability of fractional calculus will align with the region boundary and adapt to the size of the region. It will become small and narrow if the region it covers is small and narrow. This capability helps in preserving and enhancing image details, especially at the critical angle of the complicated area along the object boundary. Moreover, the combination of adaptive window and FGK, namely adaptive fractional Gaussian kernel (AFGK) provides the capability to extract the local image information, which is highly needed to extract the object boundary to avoid the local minima problem and achieve accurate segmentation.

A mixture of gradients and intensities exists near the object boundary area. Therefore, a critical part of the segmentation process is to find the exact location of contour C on the segmented object boundary to achieve accurate boundary segmentation. The gradient magnitude in the direction near the boundary may be high but it is low in the direction along the boundary or exactly on the correct boundary. Intensity inhomogeneity exists in this situation, in which the smallest image intensity pixels maybe found and randomly placed within the area. Fractional calculus can make the window narrower and smaller, such that it can adapt to the object boundary angle as it moves closer to the boundary. This technique prevents the loss of critical information and improves the classification of objects in the inhomogeneous interface. Furthermore, the proposed adaptive window with fractional calculus prevents the merging of information on the two sides of the boundary, hence keeping the intensities sharp in this area. The normal Gaussian kernel [5, 7] is represented as follows:

$$G_\alpha(x) = \frac{1}{(2\pi)^{n/2}\alpha^n} exp(-|x|^2/2\alpha^2)\,. \tag{7}$$

G_α is the Gaussian kernel where the Gaussian kernel is classified as linearity diffusion with a scale parameter of $\alpha > 0$. The two-dimensional FGK is decomposed into two one-dimensional Gaussian kernels in the proposed method, where the adaptive window is implemented. The resulting equation of one-dimensional Gaussian [28] kernel is as follows:

$$G_\alpha(x,y) = G_\alpha(x) * G_\alpha(y) \tag{8}$$

The standard deviation of the one-dimensional fractional Gaussian (σ) at a pixel should be inversely proportional to the minimum and maximum of the fractional gradient magnitude at the image pixel; thus, the standard deviations of $\sigma_x$and $\sigma_y$are represented in [28] as:

$$\sigma_x = \alpha/2(G_n + 1) \tag{9}$$

$$\sigma_y = \alpha/2(G_m + 1) \tag{10}$$

The Gaussian kernel near an object boundary becomes smaller with the increase of the local gradient. Moreover, it becomes narrower near an edge because the gradient across the edge maybe larger than the gradient magnitude along the edge. Parameter α of the Gaussian kernel in the proposed method needs to be user-tuned depending on the image characteristics. If the image is affected with high level of noise and intensity inhomogeneity, the parameter α needs to be increased to 0.5, 0.6, 0.7 or 0.8, and it should be decreased to 0.1, 0.2, 0.3 or 0.4 if the image contains low level of noise and intensity inhomogeneity. Additionally, the coordinate on both sides of the object boundary are computed to calculate the FGK with the adaptive window for an improved smoothing effect, and to obtain the relation between the points of the two sides. This computation is conducted to achieve the rotation invariance of the window using fractional calculus. The equation for this computation is given as follows:

$$R_\alpha = \Gamma(1+\alpha)\begin{pmatrix} \cos(\alpha\pi/2) & \sin(\alpha\pi/2) \\ -\sin(\alpha\pi/2) & \cos(\alpha\pi/2) \end{pmatrix} \tag{11}$$

where $R_\alpha$is the power derivative of fractional calculus with the adaptive window and α is referring to the Gaussian parameter as stated in Eq. (7). The preceding equation is further explained as follows:

$$D^\alpha \sin(t) = \sin\left(\frac{\alpha\pi}{2}\right) cos_\alpha(t) + \cos\left(\frac{\alpha\pi}{2}\right) sin_\alpha(t) \tag{12}$$

$$D^\alpha \cos(t) = \cos\left(\frac{\alpha\pi}{2}\right) cos_\alpha(t) + -\sin\left(\frac{\alpha\pi}{2}\right) sin_\alpha(t), \tag{13}$$

where D^α denotes the Riemann–Liouville fractional differential operator of the order $0 < \alpha < 1$ [29] and is given by:

$$D^\propto f(t) = \frac{d}{dt}\int_a^t \frac{(t-\tau)^{-\alpha}}{\Gamma(1-\alpha)} f(\tau) b\tau = \frac{d}{dt} I_a^{1-\alpha} f(t) \tag{14}$$

The following equation corresponds to the fractional integral operator for a continuous function *f*(t) of the order $\alpha > 0$:

$$I_a^\alpha f(t) = \int_a^t \frac{(t-\tau)^{\alpha-1}}{\Gamma(\alpha)} f(\tau) d\tau. \tag{15}$$

The rotation invariance of the adaptive window is achieved on the basis of Eqs.(12) and (13).We define the following axes by considering the fractional trigonometric function:

$$x = \Gamma(1+\alpha)[X\cos(\alpha\pi/2) - Y\sin(\alpha\pi/2) + X] \tag{16}$$

$$y = \Gamma(1+\alpha)\left[X\sin\left(\frac{\alpha\pi}{2}\right) - Y\cos\left(\frac{\alpha\pi}{2}\right) + Y\right], \tag{17}$$

where X and Y are the usual axes. The preceding relationships determine the corresponding image pixels. Furthermore, the values of the image pixel and the window are multiplied and added to obtain smooth image intensity. The advantage of using fractional calculus is obvious on the image edges and angles, which are previously ignored when a linear calculus is employed. Correspondingly, inhomogeneous object and local image information found in a given region are now effectively classified. In addition to that, the sharp edges at the boundary are maintained to improve the extraction of local information. The following section discusses the fractional-order derivative for the image segmentation process and the detailed description of the algorithm of the proposed method.

3.2 Fractional Calculus Processing

3.2.1 Energy Formulation

This section discusses on the FDH function used for extracting local image information. The FDH function is generalized using the local region-based ACM method to solve the local minima and the intensity inhomogeneity problems. We assume that a dependency exists between different image pixels and each pixel value is related to its neighbour in a region. The energy is minimized within the level set framework. We derive the following complete algorithm for the proposed method on the basis of fractional calculus:

$$\begin{aligned}&\varepsilon_\alpha^F(d_1(x), d_2(x), \phi)\\ &= \mu\int \delta(\phi(x,y))|\nabla^\alpha \phi(x,y)|dxdy\\ &+\lambda_1\int_{in} G_\alpha(x-y)|I(y)-d_1(x)|^{2*\alpha}dy \qquad 0<\alpha<1\\ &+\lambda_2\int_{out} G_\alpha(x-y)|I(y)-d_2(x)|^{2*\alpha}dy \quad 0<\alpha<1\end{aligned} \tag{18}$$

where G_α is theFGK, ∇^α is the fractional-order gradient operator, and $d_1(x)$and $d_2(x)$are the two fitting numbers placed to extract and spot the intensity which belong to the same class, as shown below:

$$d_1(\phi) = \frac{\int_\Omega I * H_x^{(\propto)}(\phi)dx}{\int_\Omega H_x^{(\propto)}(\phi)dx} \tag{19}$$

$$d_2(\phi) = \frac{\int_\Omega I * (1 - H_x^{(\propto)}(\phi)dx)}{\int_\Omega (1 - H_x^{(\propto)}(\phi)dx)} \tag{20}$$

Note that

$$\nabla^\alpha\phi(x,y) = \phi_x^{(\alpha)} + \phi_y^{(\alpha)} \tag{21}$$

We obtain the following equation using I as the image and H^{α} as the fractional differential Heaviside function:

$$H^{(\alpha)}(t-\varsigma) = H(t-\varsigma)\frac{(t-\varsigma)^{-\alpha}}{\Gamma(1-\alpha)}, \quad t > \varsigma. \tag{22}$$

The two fitting numbers are responsible in classifying and combining the inhomogeneous intensity. Both fitting numbers are placed near the intensity of the object of interest, and are used to extract the local image information embedded earlier by the Gaussian kernel. The AFGK decomposes the two-dimensional Gaussian into one-dimensional Gaussian kernel. The adaptive window is moved horizontally and vertically across the image to multiply the window and image values and produce a smooth image texture. The process is pre-calculated, saved, and reused to speed up the computations.

Parameter α in Eq.(18) represents the order of the fractional differential Heaviside function. This stage is applied within the level set framework, where stabilizing the level set is possible. The proposed method uses the FDH function instead of the integer-order gradient operator used in the previous ACM methods. The integer-order gradient operator term stands for the changing rate of the level set curve length, which is used to control the speed of the level set from shrinking. The FDH function implemented in the proposed method enables us to control the speed of the level set from shrinking, hence improves stability. The energy is minimized to complete the process of accurate boundary segmentation.

3.2.2 Energy Minimization and Level Set Method

One of the aims of the ACM is to minimize energy when the level set contour is on the object boundary. In this study, the fractional gradient descent method was used to obtain a stable contour to realize energy minimization. In any ACM methods the energy of the level set is minimized on the object boundary. For example, in the C–V method, the energy is minimized when the parameters are equal to zero, whereas the two fitting values in the LBF method are optimally chosen to minimize the energy of the level set method. Our proposed method also minimizes the energy when contour C is placed on the object boundary, with the condition that $d_i(x) \approx 0, i = 1,2$. The fractional gradient flow equation that corresponds to the FDH function and the minimization energy is defined as follows:

$$\begin{aligned} \phi_t = \ & \delta(\phi)\{\mu\,[D_x^{\alpha*}(|\nabla^{\alpha}\phi(x,y)|^{-1}D_x^{\alpha}\phi)]\} \\ & + D_y^{\alpha*}(|\nabla^{\alpha}\phi(x,y)|^{-1}D_y^{\alpha}\phi) \\ & -\lambda_1(I(y) - d_1(x))^2 + \lambda_2(I(y) - d_2(x))^2 \end{aligned} \tag{23}$$

where $D_x^{\alpha*}$ and $D_y^{\alpha*}$ are the adjoints of the usual fractional differential operator, satisfying the condition that the fractional derivative on the boundary of Ω for the function φ is vanished. The contour stops when the energy is minimized and the accurate segmentation is achieved. Based on the discussion in Sections 3.1 and 3.2, our proposed Local Fractional ACM is summarized in the following steps.

1. Initialization of contour.
2. Updating the fractional Gaussian kernel by tuning the parameter ofα, $0 < \alpha < 1$ through Eqs.(9) and (10).
3. Updating the window sizes and shapes according to the interface of intensity inhomogeneity by adjusting the α using Eqs.(12) and (13).
4. Updating the fitting numbers, $d_1(x)$ and $d_2(x)$ optimally using Eqs. (19) and (20), respectively.
5. Evolving the level set function according to Eq. (23).
6. Regularizing and minimizing the energy of the level set function.
7. When the condition of $d_i(x) \approx 0, i = 1,2$ is met, the contour movement is stopped; otherwise, return to step 2.

4.0 EXPERIMENTAL RESULT AND DISCUSSION

The experiment in this study was designed using Matlab R(2008b) on a 2.5 GHz Intel Processor i5 according to the implementation framework. The experiments were divided into two parts: 1) Benchmarking Evaluation and 2) Quantitative Evaluation. Both synthetic and medical images with severe intensity inhomogeneity problem were used in both parts of the experiments. The medical dataset used in both experiments comprises of 2D images derived from the image clef database from year 2010 to 2012.

4.1Benchmarking Evaluation

The benchmarking evaluation was conducted to measure the effectiveness of the proposed method in handling accurate boundary segmentation in the presence of severe intensity inhomogeneity interface. The performance of our proposed method is compared with other three different ACM methods that rely on local image information for their segmentation processes. These methods are Local Gaussian Method (LGD) [27], Local Intensity Clustering (LIC) [26], and Local Binary Fitting Energy (LBF) [7]. In the first experiment, a synthetic image of a star affected with intensity inhomogeneity was presented. Three images of a star with different levels of intensity were provided. Notably, the object of the star is placed within a blank or white background without any intensity. In the first column, the image of a star is totally black. The second column depicts the star image with intensity inhomogeneity, in which the distribution of intensity gradually decreases from top to bottom, however the gradient magnitude remains visible and is not considered as low. Meanwhile, the star image in the last column was affected with severe intensity inhomogeneity, where the gradient magnitude decreases from top to bottom and has a very low gradient magnitude at the bottom of the object. Given this situation, the gray intensity is less observed especially at the boundary of the object, thus may result in an inaccurate segmentation.

Fig. 3 depicts the results obtained from the experiment. The first row of Fig. 3 illustrates the segmentation results obtained using the LGD method, followed by the LIC method in the second row, the LBF method in the third row and the last row represents our segmentation outcome on the star image with severe intensity inhomogeneity problem. For the star image in the first and second columns, our method demonstrates accurate boundary segmentation because the contour stopped exactly on the boundary of the object to be segmented. This indicates that the level set method (LSM) is regularized and the contour C meets the condition $d(t) \approx 0$ which enables it to stop exactly on the object boundary.

Meanwhile, the anti-aliasing problem of the star image in the first column forced the contours of both the LGD and LBF methods to deviate slightly from the object boundary. Nonetheless, the LIC method managed to segment the star accurately on its exact boundary (first column, second row). Better segmentation outcomes were obtained on the star images in the second column as compared to the other columns. Aside from the LGD segmentation result, other methods including the proposed method, produce accurate boundary segmentation. In the LIC method, the clustering technique proposed succeeded in clustering and grouping the intensity together, thereby regularizing the level set when the condition is met. Similar to LBF, the fitting energy applied allocates the intensity that fit at the boundary to regularize the level set function and force the contour to stop exactly at the correct boundary. The same experiment was repeated on the last star image (third column). The lower part of the image is having a very low gradient magnitude and severely affected by intensity inhomogeneity, posing a great challenge to the segmentation process. Given this characteristic, all the baseline methods applied in this experiment failed to segment the image completely. The contour stopped halfway through the image as the gradient magnitude became lesser and almost disappeared into the background. On the contrary, our method managed to complete the segmentation process with exact boundary accuracy. Given that the image is severely affected by intensity inhomogeneity problem, the parameter used should be adjusted and increased to eight for enhanced smoothness.

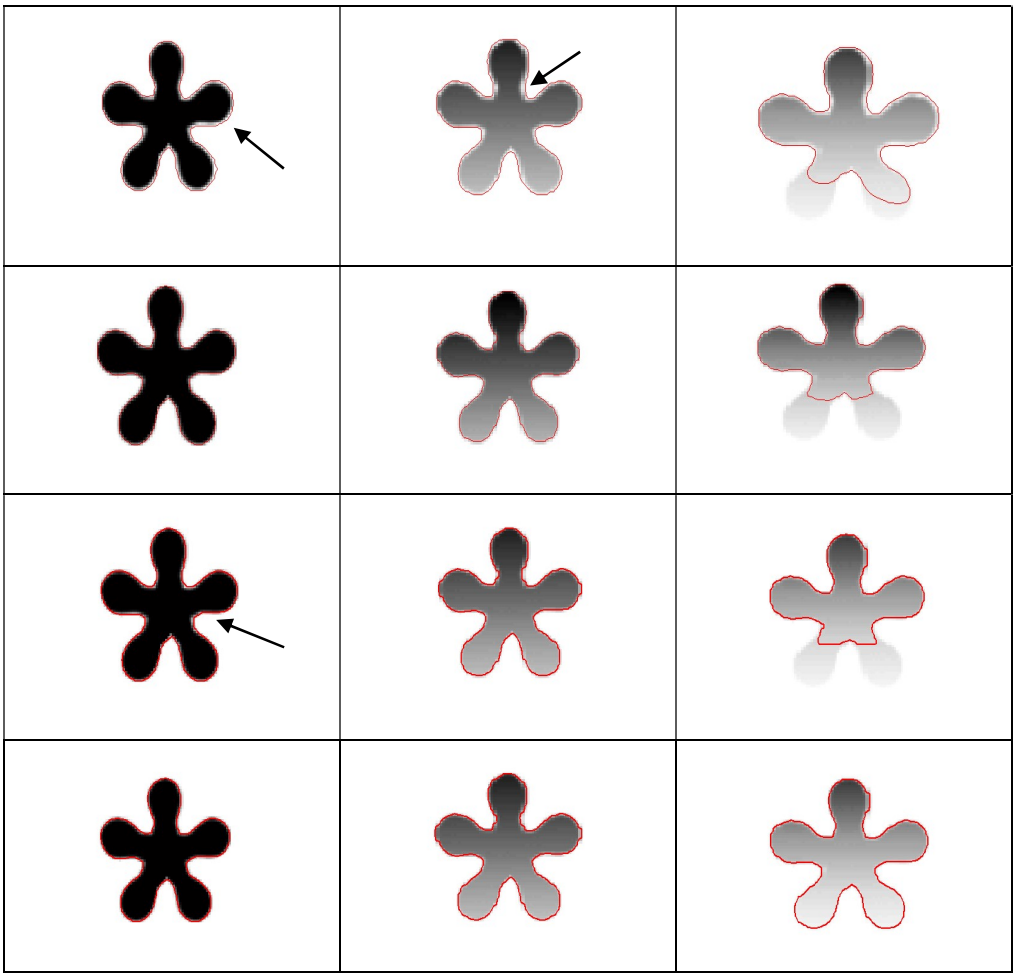

Fig. 3: Segmentation results of the three synthetic images of a star with different levels of intensity. The first row shows the result obtained by LGD method, the second row shows the result by LIC method, the third row shows the result obtained by LBF method, and the last row shows the result obtained by our method for α=0.1(first column), α=0.1 for second column and α=0.5 for the last column.

The successful segmentation outcome was made possible because a novel implementation of AFGK was provided to sustain the lower frequency of the image and to enhance its edges. At the boundary of the object where the gradient magnitude is difficult to observe and from where the local minima problems originate, the local image information embedded by the Gaussian kernel is extracted by the FDH function, which searches into the gradient and the intensity in the image. At this situation, the two numbers, d_1 and d_2 (Eq. 18), placed near the intensity surrounding the object boundary extracts the intensity and the gradient. The parameter of the Gaussian kernel is adjusted to become larger hence, the smoothness of the contour evolution could be made faster and the level set contour may shrink. Meanwhile, the FDH function controls the speed of a contour during its evolution and maintains its stability. Our experiment was continued with another synthetic image of a flower on a black background to investigate the performance of our method against other baseline methods when a bright object on a darker background is used.

Fig. 4(a) shows the result using the LGD method followed by the LIC method segmentation outcome in Fig. 4(b), the LBF segmentation outcome in Fig. 4(c), and our method in Fig. 4(d). The results demonstrated different outcomes. Notably, the flower image has a sharp boundary toward its centre. The LGD and LIC methods did not manage to segment the inward boundary accurately, as indicated by the arrows. Meanwhile, the LBF method was completely unsuccessful in segmenting the image completely because of the sensibility of the two contour

placements by the method. Our method outperformed the others with complete and accurate boundary segmentation of the flower even on its inward boundary. This finding proves that our method has the capability to focus on and maintain tiny image details, and has a potential to segment the object boundary accurately even at sharp and tiny curves as in the case of the flower. This process is accomplished with the use of AFGK to get a smoother image texture and the FDH to extract the local image information for better segmentation outcome. The adaptive window used could move within the critical angle (inward of the flower object) and enables the FDH function to extract the accurate boundary. Therefore, in the experiments shown in Figures III and IV, our method could realize accurate boundary segmentation within an interface of severe or normal intensity inhomogeneity regardless the situation of both the background and foreground intensities.

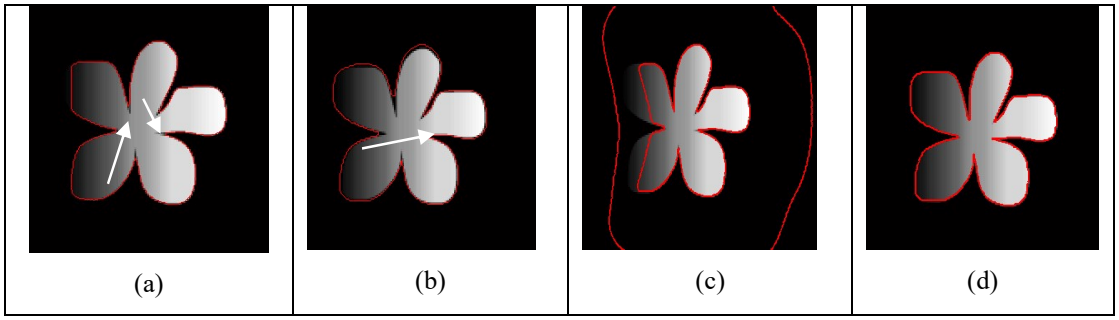

Fig. 4: Segmentation results on synthetic image of a flower where the background intensity is a solid black. The first column shows the result by the LGD method, the second column shows the result by the LIC method, the third column results are obtained by the LBF method, and the results in the last column are obtained on the basis of our method for α=0.6.

The remainder of our experiments aim to validate our positive experimental results using real medical images with more challenging texture and structure. The medical images used in the experiments are MRI, CT scan, microscopic and x-ray images. The same ACM baseline methods that utilize local image information in their segmentation process were used for comparison. Our experiment began with an MRI image of the brain. The internal part of the brain image contains white flares with inhomogeneous intensity. Unlike other images, the white flare is thin, with long and winding structure.

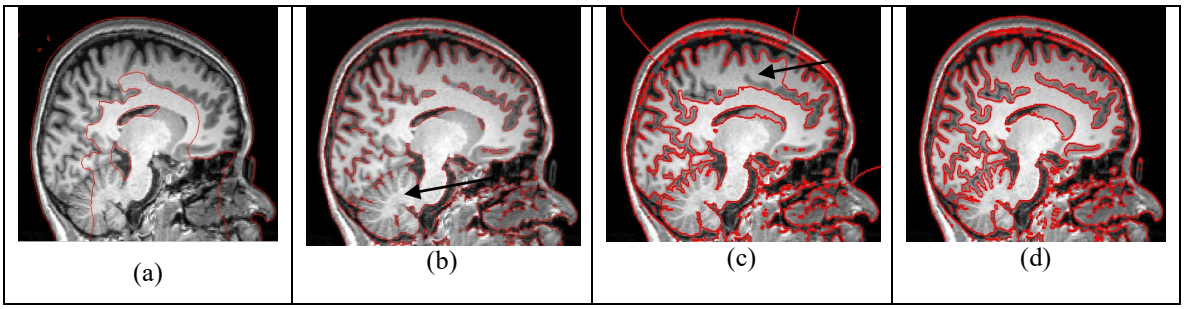

Fig. 5: Segmentation results on MRI image of a brain. The first column shows the result by the LGD method, the second column shows the result by the LIC method, the third column results obtained by the LBF method, and the last column shows the result obtained on the basis of our method for α=0.6.

Fig. 5 presents the results obtained from the experiment conducted on the MRI image of a brain. Fig. 5(a) shows the segmentation outcome using the LGD method followed by the LIC method in Fig. 5(b), the LBF segmentation

outcome in Fig. 5(c) and our method in Fig. 5(d). The LGD method did not manage to segment the internal part of the brain. Its contour failed to be placed along the object boundary of the white flare areas, thus hinders inaccurate segmentation. Likewise, the LIC method was also not successful in accurately segmenting the brain structure within the white flare area, as indicated by the arrow as shown in the Fig. 5(b). The LBF method is sensitive to the initial placement of its contour hence, the object boundary of the white flare is also not well segmented. This failure may be due to the two contours on the image. Some parts of the object boundary were not segmented, as indicated by an arrow in Fig. 5(c). In addition, the method also showed slight over sampling effect in its outcome. In this situation, accurate segmentation could not be achieved. Meanwhile, our method managed to produce a comprehensive and accurate boundary segmentation outcome successfully even in white flare areas. The capability to manoeuvre segmentations along the complex brain structure which is long and winding with sharp curves, is mainly attributed to its novel AFGK and FDH function. The AFGK technique provides a smooth texture yet preserves critical information such as the edges at some critical part, such as the white flare. In this situation as the level of intensity inhomogeneity of the internal part is slightly higher, the value of α is tuned to 0.6. The adaptive window supports the Gaussian kernel by moving towards critical angles along the boundary of the white flare, hence enabling the FDH function to extract the intensity at that position and regularize the level set.

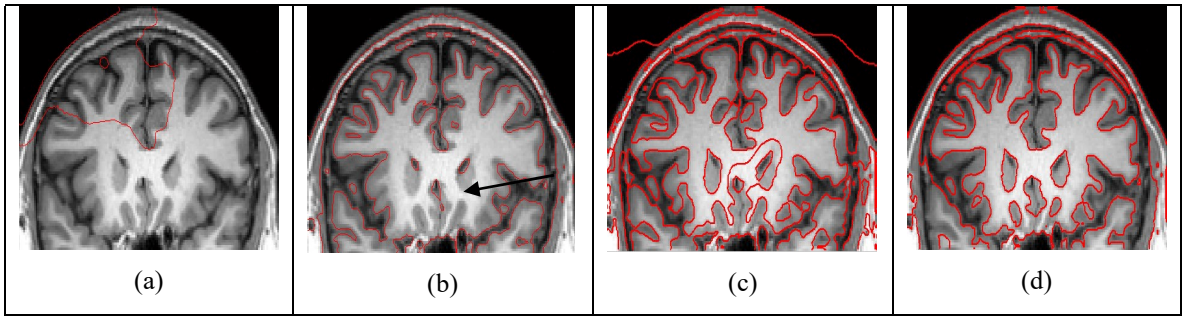

Fig. 6: Segmentation results on another MRI image of brain from the top view. The first column shows the result by the LGD method, the second column shows the result by the LIC method, the third column results obtained by the LBF method, and the last column shows the result obtained on the basis of our method for α=0.6.

The same experiment was repeated on another slice of an MRI image that shows the top view of the brain, with more focus given to the white flare areas as shown in Fig. 6. This experiment was conducted to support the previous experiment. The α is also tuned to 0.6 as the characteristics of the image is similar to the previous one. An improved segmentation outcome was obtained with the second experiment compared to the first experiment. As expected, the segmentation result was consistent with the previous experiment for all tested methods. The LGD method still failed to complete the segmentation process successfully because of the severe intensity inhomogeneity in the image. The LIC method produced a better segmentation outcome, but failed to segment the brain structures situated in the white flare areas, as indicated by the arrow in Fig. 6(b). Meanwhile, the LBF method managed to segment almost all the brain structure, but with less accuracy and has a slight tendency to segment unwanted regions. Our method shows satisfactory results and achieved accurate boundary segmentation, similar to the outcome depicted in Fig. 5. To prove the good collaboration of AFGK and FDH, the next experiment was conducted on a CT SCAN image of a brain. Fig. 7 illustrates the outcome obtained based on the experiment conducted using the four methods of ACM including FGH ACM method.

Fig. 7 depicts the outcome based on LGD method at Fig. 7(a), followed by the outcome using the LIC method at Fig. 7(b), outcome by the LBF method is presented at Fig. 7(c) and the outcome based on our proposed method at Fig. 7(d). The modality of CT scan image shows a dark area at the inner part of the brain with least intensity. Therefore, the α is tuned to 0.8. Most white flare was affected with least intensity which causes the white flare boundary to be disappeared due to the darkness of the image texture. Due to the darkness factor, LGD method did not manage to complete the segmentation where the contour could not segment the white flare area situated at the inner part of the brain.

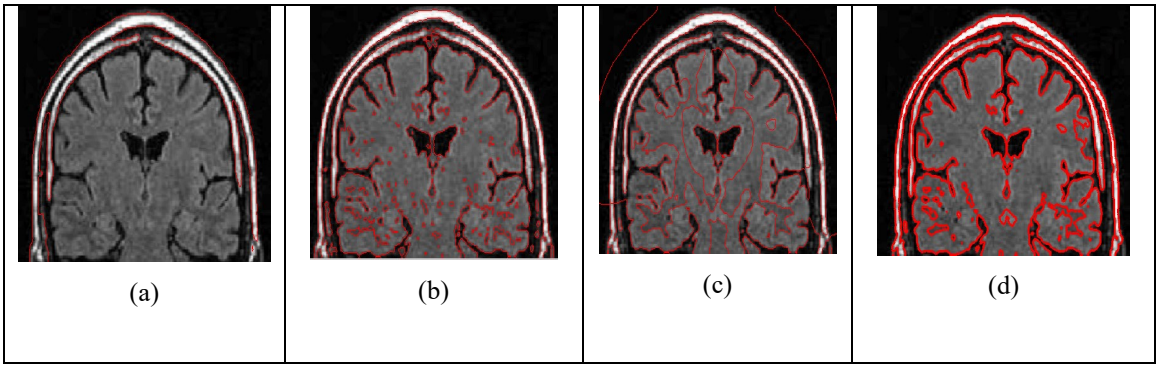

Fig. 7: Segmentation results on another brain image but using CT SCAN modality. (a) shows the result by LGD method, (b) shows the result by LIC method, (c) is the results obtained by LBF method, and (d) is the result obtained on the basis of FGH ACM method for α=0.8.

The LBF method managed to move the contour at the inner part, however the contour did not manage to produce an accurate segmentation as shown Fig. 7(c). This may be due to the sensibility of the two contour placement of the method. On the other hand, the LIC and the proposed method managed to segment the inner part of the brain. Having said that, the LIC method was still facing inaccuracy in the segmentation where it produced over sampling problems as shown in Fig. 7(b). Our proposed method shown at Fig. 7(d) managed to provide accurate segmentation with lessen over sampling with parameter of α= 0.9. This proves that the collaboration between AFGK and FDH provide an accurate boundary segmentation of the proposed method.

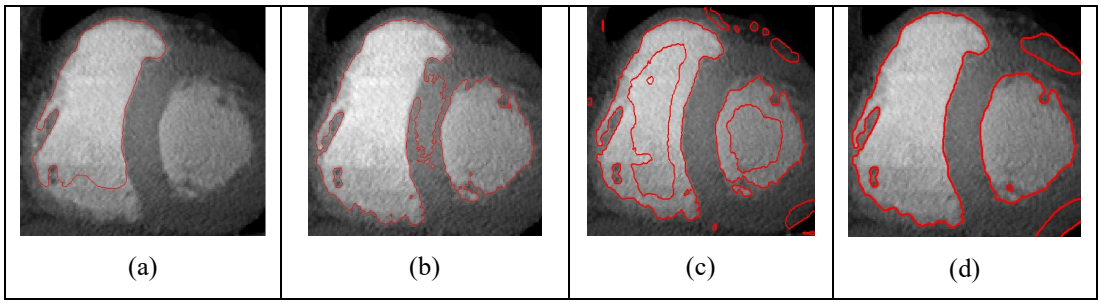

Fig. 8: Segmentation results on a heart image of CT SCAN. (a) shows the result by LGD method, (b) shows the result by LIC method, (c) shows the results obtained by LBF method, and (d) shows the result obtained by our method for α=0.8.

Next finding reports on a CT scan image of a heart which is then followed by another image of heart using the modality of MRI. Both heart images have soft texture with severe inhomogeneous intensity. The objects to be segmented in Fig. 8 have lighter intensity and are located in the sub-region of the object.

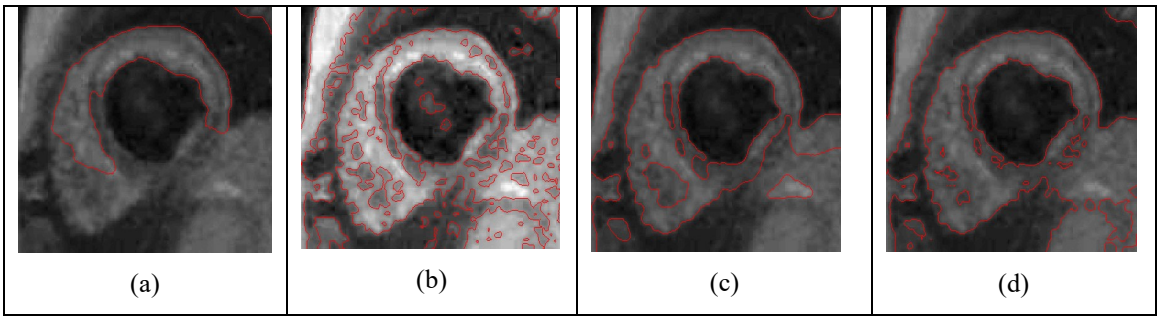

Fig. 9: Segmentation results on a heart image of CT SCAN. (a) shows the result by LGD method, (b) shows the result by LIC method, (c) shows the results obtained by LBF method, and (d) shows the result obtained by our method for α=0.9.

Fig. 8 shows the result obtained using the LGD method, followed by those obtained through the LIC, LBF and the proposed methods respectively in Fig. 8 (a), (b), (c) and (d). Among the presented results, the proposed method shows significant improvement in the segmentation outcome, accurately segmenting the boundary of the two objects successfully with α = 0.8. Other methods, such as the LGD method, did not manage to segment the object where only one object is segmented. The objects are not well segmented by LBF because of the sensibility problem of the contour. The LIC method managed to show some segmentation however, the result obtained was neither accurate nor satisfying, demonstrating some over sampling effects. To prove the effectiveness of the proposed method, another heart image from the modality of MRI is used. Its texture is soft but the image is darker than one in CT scan image. The boundary of heart is affected by lots of noise which leads to intensity inhomogeneity thus making the segmentation process crucial.

Fig. 9 (a), (b), (c) and (d) shows the result obtained using the LGD method, followed by those obtained through the LIC, LBF and the proposed methods. Similar as the previous outcome, the proposed method depicted the most perfect outcome with better accuracy at the object boundary and cleaner outcome for α=0.9 as the image is slightly darker than the image in Fig. 8. The LGD and LBF method did not manage to segment some part of the object boundary. On the other hand, the LIC method managed to complete the segmentation but produced over sampling.

The next experiment presents images by x-ray modality of blood vessels. It is known that the object of blood vessels is long, thin and winding. The image has high level of noise and the distribution of intensity is not homogeneous. In addition the level of intensity of the object of interest is at least until it made it difficult to be separated from the background. Due to this factor the αis tuned to 0.8. This is shown in Fig. 10.

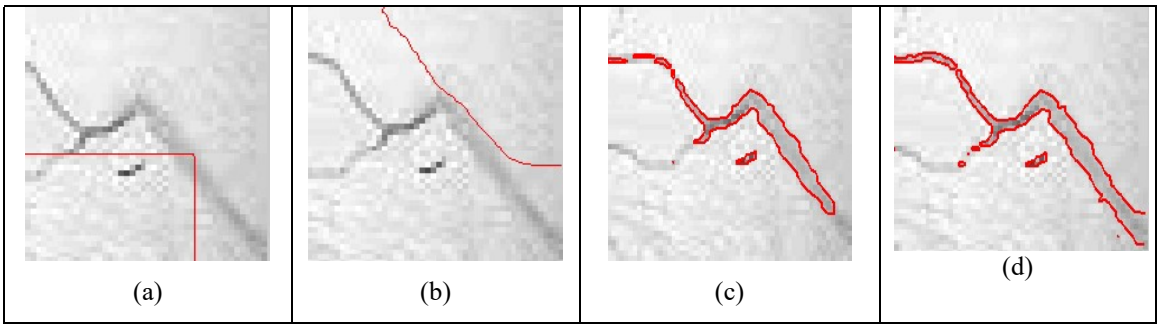

Fig. 10: Segmentation results on blood vessel from x-ray modality. (a) shows the result by LGD method, (b) shows the result by LIC method, (c) is the results obtained by LBF method, and (d) shows the result obtained on the basis of our method for α=0.8.

The pixel intensity within the neighbourhood pixels inside the blood vessel has similar levels which lead to over sampling during the segmentation process. The results obtained by the four methods denote various segmentation outcomes and these are shown in Fig. 10 (a),(b),(c) and (d). Both the LGD and LIC methods completely failed to segment the object in this image, indicating the inability of their contours to evolve in the environment severely affected by intensity inhomogeneity problem. Meanwhile, the LBF method and the proposed method were able to move the contour along the blood vessel and produce better segmentation outcomes. Nonetheless, the outcome of the proposed method is more complete and accurate than those produced by the LBF method for $\alpha = 0.8$ as shown in Fig. 10(d).

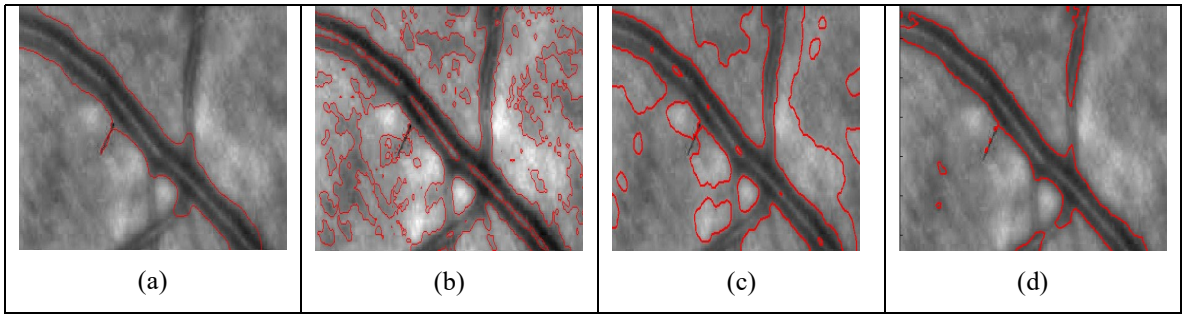

Fig. 11: Segmentation results on blood vessel of an eye taken from x-ray modality. (a) shows the result by LGD method, (b) shows the result by the LIC method, (c) is the results obtained by LBF method, and (d) shows the result obtained on the basis of our method for α=0.9.

Another x-ray image of blood vessel is shown in Fig. 11 that depicted an object of blood vessel which is dark with noise and intensity inhomogeneity. The results obtained were depicted in Fig. 11 (a), (b), (c) and (d) which shows a slightly different outcome from those in Fig. 10. This is due to the image texture which is darker and having intensity inhomogeneity at the foreground. As the blood vessels is having similar intensity in the pixel neighbourhood, the LGD method Fig. 11(a) and LBF method at Fig. 11(c) shows over sampling at the inner part of the blood vessels. This means both methods does not managed to provide a successful segmentation, On the other hand, the proposed method and LGD method show good segmentation results as before. Nonetheless, the outcome of the proposed method is more complete and accurate than those produced by the LGD method with $\alpha = 0.9$.

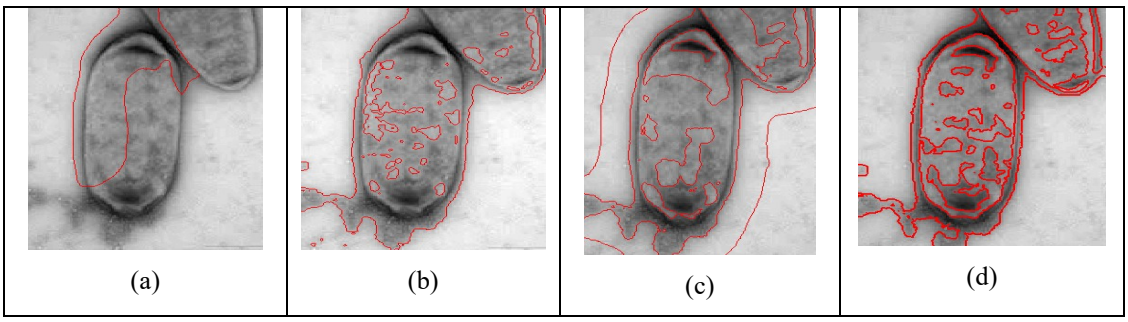

Fig. 12: Segmentation results on microscopic image of bacteria. (a) shows the result by LGD method, (b) shows the result by LIC method, (c) is the results obtained by LBF method, and (d) shows the result obtained on the basis of our method for α=0.8.

The last experiment conducted in this section was on microscopic images of bacteria. Both images are shown in Fig. 12 and Fig. 13 respectively. Note that, the microscopic images of bacteria are having bacteria object with the least intensity and yet the background is also having a similar intensity as the one in the object. The intensity distribution is not well distributed which made the segmentation failed to be completed or produce over sampling. The object of bacteria as shown in Fig. 12 is having several level of intensity that leads to over sampling. This is shown by the outcome of the image using the four methods mentioned earlier.

Fig. 12(a) depicted the outcome using the LGD method, outcome from LIC method at Fig. 12 (b), outcome from LBF method at Fig. 12 (c) and the proposed method at Fig. 12(d). Notice that LGD method and LIC method could not produce satisfying segmentation, where the actual object of bacteria is not really segmented, shown by the arrow. On the other hand, both the LBF and the proposed method managed to complete and perfectly segment the bacteria object from the background, with some over sampling. Nonetheless, the outcome by the proposed method is better without any over sampling at the background of the image compared the other methods for α=0.8. To support the outcome as in Fig. 12, another microscopic image of bacteria was used with similar characteristic as above and is shown in Fig. 13. This time, the object of bacteria was affected with intensity inhomogeneity along the object boundary until the boundary is having gaps along the boundary.

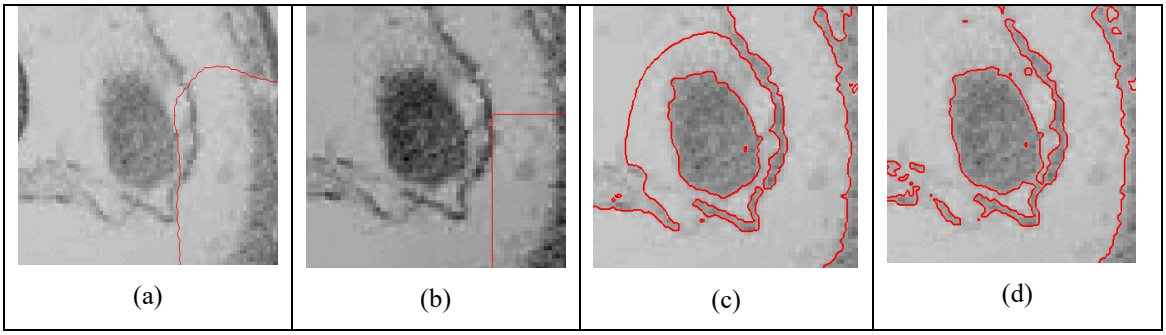

Fig. 13: Segmentation results on microscopic image of cell. (a) shows the result by the LGD method, the second column shows the result by the LIC method, results obtained by the LBF method, and the last column shows the result obtained on the basis of our method for α=0.8.

Fig. 13 depicted the results gained from the experiment conducted. Fig. 13(a) is the result obtained from LGD method, Fig. 13(b) is the result obtained from LIC method, Fig. 13(c) is the result from LBF method and Fig. 13(d) is the result obtained from the proposed method. From the results presented, it is obvious that, the contour of the LGD and LIC methods could not move toward the object of interest, thus failing the segmentation. The method by LBF and the proposed method managed to move the contour toward the object of interest and provide satisfying result. However, the LBF produce some over sampling. Besides the benchmarking evaluation, a quantitative evaluation is also conducted in this work. The quantitative evaluation is based on work by Abbas et al [4] and the result is presented in the next section.

4.2 Quantitative Evaluation

To support the experimental findings, a quantitative evaluation was also conducted. The quantitative evaluation is based on evaluation metric [4]. There are three types of evaluations which are specificity, sensitivity and accuracy [4]. However, in this work we only focus on the accuracy metric. To conduct the evaluation, two images of the same medical image were used. The first image was the segmented image produced by each of the selected ACM methods including ours. The second image is the medical image with manually drawn boundary. The accuracy of the segmentation outcome is evaluated by measuring the distance of the manually drawn boundary to the automatic boundary created by the ACM methods. Let B be the automatic border, H be the manually drawn border and *d* is the distance between B and H. Thus the equation of *d* is given as;

$$d(B,H) = argm \quad (b_s, h_t), b_s \in B,\ h_t \in H \tag{24}$$

To get the percentage of the segmentation accuracy metric q is computed as the rate of minimum distance between both manual and automatic borders. The metric q is computed as;

$$q = \frac{nd}{s}\ x\ 100\% \tag{25}$$

The higher the percentage of accuracy depicted that the border of the segmentation is near at the object boundary.Table I shows the result of the quantitative evaluation process. The result shows that the proposed method provides accurate boundary segmentation on most of the medical images as compared to other baseline methods. It provides an average accuracy of 94.85% whereas the LGD method provides the average accuracy of 63.29%, the LIC method provides the average accuracy of 75.09% and the LBF method provides the average accuracy of 91.75%. The metric of accuracy shown in Table I is aligned with the segmentation outcomes from the earlier benchmarking evaluation process.

Table 1. The evaluation metric comparison for medical images among LGD, LIC, LBF and FGH ACM method.

Medical images	**Metric of Accuracy**			
	LGD	**LIC**	**LBF**	**Proposed Method**
MRI image of brain 1	72.23	89.48	90.23	97.51
MRI image of brain 2	70.86	92.49	94.31	97.88
CT SCAN image of brain	71.45	94.04	94.92	96.11
CT SCAN image of heart 1	65.48	92.08	93.44	95.71
CT SCAN image of heart 1	86.76	91.89	91.11	94.23
X-ray image of blood vessel 1	23.11	21.07	91.87	93.49
X-ray image of blood vessel 2	90.41	86.01	88.09	91.88
Microscopic image of bacteria 1	67.12	87.72	89.16	92.45
Microscopic image of bacteria 2	22.23	21.1	92.63	94.39

5.0 CONCLUSION

In this study, a novel local region-based active contour model with fractional calculus for medical image segmentation in the presence of intensity inhomogeneity was presented. The proposed method improves the extraction of local image information in order to achieve accurate boundary segmentation on multimodality of medical images that contain high level of noise and intensity inhomogeneity. The proposed method comprises of two important components: Adaptive Fractional Gaussian Kernel (AFGK) and Fractional Differentiate Heaviside (FDH). The AFGK is comprises of fractional Gaussian Kernel (FGK) and adaptive window mechanism. Our investigation shows that the collaboration between the fractional calculus and nonlinear Gaussian Kernel (FGK) extends the capability of the nonlinear Gaussian in preserving edges in an image through the process of merging and

grouping the homogeneous object in the same regions. The FGK also protect the edges for easy extraction by the FDH function. The FDH function is responsible for extracting the local image information as it weighs not only the gradient but also the intensity of the image. Additionally, the fractional order gradient of FDH is capable in controlling the speed of a contour from shrinking thus maintain its stability. The collaboration of AFGK and FDH provides excellent result in producing accurate boundary segmentation on multimodality of medical images with different anatomical structures even in the presence of high level of intensity inhomogeneity. The benchmarking evaluation shows that the proposed method produces accuracy of segmentation along the object boundary when compared to the LBF, LGD and LIC methods. The quantitative evaluation also demonstrates a successful segmentation outcome with above 90% accuracy.

REFERENCES

[1] J. Ning, L. Zhang, D. Zhang and C. Wu, Interactive image segmentation by maximal similarity based region merging, Pattern Recognition 43 (2010) 445–456.

[2] S. Naji , R. Zainuddin , H. A. Jalab, Skin segmentation based on multi pixel color clustering models. Journal of Digital Signal Processing, 22(6)(2012) 933- 940. DOI:10.1016/j.dsp.2012.05.004

[3] K. Zhang, Q. Liu, H. Song, and X. Li, A variational approach to simultaneous image segmentation and bias correction., IEEE Trans. Cybernetics, 2014.

[4] A. A. Abbas, X. Guo, W. Tan, H. A. Jalab, Combined Spline and B-spline for an improved automatic skin lesion segmentation in dermoscopic images using optimal color channel. Journal of Medical Systems, 38 (8)(2014) 1-8, DOI 10.1007/s10916-014-0080-7.

[5] C. Li, R. Huang, Z. Ding, J. C. Gatenby, D. N. Metaxas, John C. Gore, A Level Set Method for Image Segmentation in the Presence of Intensity Inhomogeneitiesm With Application to MRI, IEEE Transactions On Image Processing, 20(7)(2011).

[6] C. Jagath, Rajapakse, F.Kruggel, Segmentation of MR images with intensity inhomogeneities, Image and Vision Computing 16 (1998) 165–180.

[7] C. Li 1, C.Y Kao, John C. Gore, and Z. Ding, Implicit Active Contours Driven by Local Binary Fitting Energy, IEEE Transactions on Image Processing, 2007

[8] M. Kass and A. Witkin, and D. Terzopoulos, Snakes: Active contour models, International Journal of Computer Vision 1 (1987) 321–331.

[9] V. Caselles, R. Kimmel, G. Sapiro, “Geodesic active contours”, in: Processing of IEEE International

Conference on Computer Vision'95. Boston, MZ, 1995, pp. 694–699.

[10] V. Caselles, R. Kimmel, G. Sapiro, "Geodesic active contours", International Journal of Computer Vision, 22(1) (1997) 61-79.

[11] C. Li, C. Kao, J. C. Gore and Z. Ding, "Minimization of region-scalable fitting energy for image segmentation," IEEE Trans. Image Process., 17(10)2008) 1940-1949.

[12] T. Chan, L.Vese, Active contour without edges", IEEE Trans on Image Processing 10 (2) (2001) 266-277.

[13] D. Tian, D. Xue, D. Chen, S. Sun, A Fractional-order Regulatory CV Model for Brain MR Image Segmentation, Control and Decision Coference, 2013, China

[14] P. Ghamisi, Michael S. C, J.A Benediktsson, Nuno M.F.,An efficient method for segmentation of images based on fractional calculus and natural selection, Expert Systems with Applications 39 (2012) 12407–12417

[15] D. Mumford, J. Shah, Optimal approximation by piecewise smooth function and associated variational problems, Communications on Pure and Applied Mathematics 42 (1989) 577–685.

[16] X. Bresson, S. Esedoglu, P. Vandergheynst, J. Thiran, S. Osher, Fast global minimization of the active contours/Snakes model, Journal of Mathematical Imaging and Vision 28 (2007) 151–167.

[17] S. Osher and J. Sethian, Fronts propagating with curvature dependent speed: Algorithms based Hamilton-Jacobi formulations, Journal of Computational Physics 79 (1988) 12–49.

[18] T. Brox, D. Cremers, On Local Region Models and a Statistical Interpretation of the Piecewise Smooth Mumford-Shah Functional, International Journal of Computer Vision 84 (2009) 184–193.

[19] A. Vasilevskiy and K. Siddiqi, Flux-maximizing geometric flows, IEEE Transaction on Pattern Analysis and Machine Intelligence 24 (2002) 1565–1578.

[20] S. Lankton, A. Tannenbaum, Localizing Region-Based Active Contours, IEEE Transactions on Image Processing 17 (2008) 2029–2039.

[21] K. Zhang, H. Song, and L. Zhang, Active contours driven by local image fitting energy, Pattern recognition

43 (2010) 1199–1206.

[22] K. Zhang, L. Zhang and S. Zhang, A variational multiphase level set approach to simultaneous segmentation and bias correction, IEEE International Conference on Image Processing (2010) 4105–4108.

[23] C. Darolti, A. Mertins, C. Bodensteiner, and U. Hofmann, Local region descriptors for active contours evolution, IEEE Transactions on Image Processing 17 (2008) 2275–2288.

[24] M. A. Shayegan, S. Aghabozorgi, and R. G. Raj, "A Novel Two-Stage Spectrum-Based Approach for Dimensionality Reduction: A Case Study on the Recognition of Handwritten Numerals," Journal of Applied Mathematics, vol. 2014, Article ID 654787, 14 pages, 2014. doi:10.1155/2014/654787.

[25] Reena S.,V. K. Srivastava, Weighted non-linear diffusion filtering with wavelet thresholding in image denoising, International Journal of Computer Applications (0975 – 8887) Volume 78 – No.14, September 2013.

[26] C. Li, R. Huang, Z. Ding, C. Gatenby, D. Metaxas, and J. C. Gore, A Level Set Method for Image Segmentation in the Presence of Intensity Inhomogeneities with Application to MRI, IEEE Transactions on Image Processing 20 (2011) 2007–2016.

[27] L. Wang, L. He, A. Mishra, C. Li, Active contours driven by local Gaussian distribution fitting energy, Signal Processing 89 (2009) 2435–2447.

[28] Ardeshir Goshtasby, Martin Satter, An adaptive window mechanism for image smoothing, Computer Vision and Image Understanding 111 (2008) 155–169.

[29] Gerd Baumann, Frank Stenger, "Fractional Calculus and Sinc Methods", Fractional Calculus and Applied Analysis, December 2011, Vol.14, Issue 4, pp 568 – 622.